TOR signaling regulates planarian stem cells and controls localized and organismal growth

T. Harshani Peiris[1,2], Frank Weckerle[1], Elyse Ozamoto[1], Daniel Ramirez[1], Devon Davidian[1], Marcos E. García-Ojeda[1] and Néstor J. Oviedo[1,*]

[1]Department of Molecular and Cell Biology, School of Natural Sciences, University of California at Merced, 5200 North Lake Road, Merced, CA 95343, USA
[2]Quantitative and System Biology, Graduate Program University of California at Merced, 5200 North Lake Road, Merced, CA 95343, USA
*Author for correspondence (noviedo2@ucmerced.edu)

Accepted 13 February 2012
Journal of Cell Science 125, 1657–1665

doi: 10.1242/jcs.104711

Summary

Target of Rapamycin (TOR) controls an evolutionarily conserved signaling pathway that modulates cellular growth and division by sensing levels of nutrients, energy and stress. As such, TOR signaling is a crucial component of tissues and organs that translates systemic signals into cellular behavior. The ubiquitous nature of TOR signaling, together with the difficulty of analyzing tissue during cellular turnover and repair, have limited our understanding of how this kinase operates throughout the body. Here, we use the planarian model system to address TOR regulation at the organismal level. The planarian TOR homolog (*Smed-TOR*) is ubiquitously expressed, including stem cells (neoblasts) and differentiated tissues. Inhibition of *TOR* with RNA interference severely restricts cell proliferation, allowing the study of neoblasts with restricted proliferative capacity during regeneration and systemic cell turnover. Strikingly, TOR signaling is required for neoblast response to amputation and localized growth (blastema). However, in the absence of TOR signaling, regeneration takes place only within differentiated tissues. In addition, *TOR* is essential for maintaining the balance between cell division and cell death, and its dysfunction leads to tissue degeneration and lack of organismal growth in the presence of nutrients. Finally, TOR function is likely to be mediated through TOR Complex 1 as its disruption recapitulates signs of the TOR phenotype. Our data reveal novel roles for TOR signaling in controlling adult stem cells at a systemic level and suggest a new paradigm for studying TOR function during physiological turnover and regeneration.

Key words: Regeneration, Stem cells, Planarian, TOR

Introduction

Target of Rapamycin (TOR) is an evolutionarily conserved kinase that modulates cell division and growth in response to energy and nutrient levels (Wullschleger et al., 2006; Russell et al., 2011; Zoncu et al., 2011). TOR functions as an endogenous sensor that directs the behavior of cells across different tissues. Dysfunctional TOR signaling has been implicated in a range of systemic complications, including cancer, degenerative disease and aging (Wullschleger et al., 2006; Zoncu et al., 2011). Studies in vertebrate and invertebrate models revealed TOR as a crucial stem cell regulator, but the mechanism by which this pathway controls cellular behavior across the adult body remains poorly understood (Oldham et al., 2000; Murakami et al., 2004; LaFever et al., 2010; Russell et al., 2011). This limitation is twofold: (1) TOR inactivation results in embryonic lethality in both vertebrates and invertebrates, making the study of its roles in adults more challenging, and (2) the ubiquitous nature of TOR signaling, together with the difficulty of analyzing tissue turnover in vivo, restricts our ability to dissect TOR regulation at the systemic level (Russell et al., 2011; Zoncu et al., 2011).

The adult planarian *Schmidtea mediterranea* is an excellent model organism with which to address roles of TOR in regulating cell behavior at an organismal level. Planarians possess an abundant and accessible somatic stem cell population (neoblasts) that maintain differentiated tissues throughout the body, remarkable evolutionary conservation of signaling pathways, and well-characterized regenerative ability (Reddien and Sánchez Alvarado, 2004; Gentile et al., 2011).

We report the identification of a TOR homolog ubiquitously expressed in *S. mediterranea* (*Smed-TOR*, abbreviated to *TOR*). RNA interference (RNAi) of *TOR* disrupts neoblast behavior at the systemic level. Furthermore, TOR signaling is an essential component of the neoblast response to damage and tissue turnover. Strikingly, amputated *TOR(RNAi)* animals regenerate nervous system tissue within the pre-existing tissue. *TOR* is crucial for maintaining the balance between cell division and cell death, which is fundamental during adult tissue turnover. Additional analysis using RNAi suggests that TOR phenotype is mediated by TOR complex-1 (TORC1). Taken together, we propose the use of *S. mediterranea* as a powerful model system that could be used to provide insights into the roles TOR signaling plays at the organismal level during systemic tissue turnover and regeneration.

Results and Discussion

A TOR homolog exists in *S. mediterranea* and is expressed in stem cells and differentiated tissues

TOR is a highly conserved protein kinase among eukaryotes. We identified a single TOR member in the *S. mediterranea* genome (*Smed-TOR*, abbreviated to *TOR*) with unique signature domains

(supplementary material Fig. S1). Whole-mount in situ hybridization (ISH) showed *TOR* expression to be widely distributed throughout the planarian body except the pharyngeal area (Fig. 1A). Experiments with *TOR* sense and antisense probes on *TOR(RNAi)* animals (see below) confirmed the specificity of the expression (Fig. 1B,C). To characterize further the cell types expressing *TOR*, ISH experiments were carried out on cells isolated by fluorescence-activated cell sorting (FACS) (Fig. 1D–G). These experiments revealed that *TOR* expression is present in the majority of proliferative neoblasts (X1 cells), in their

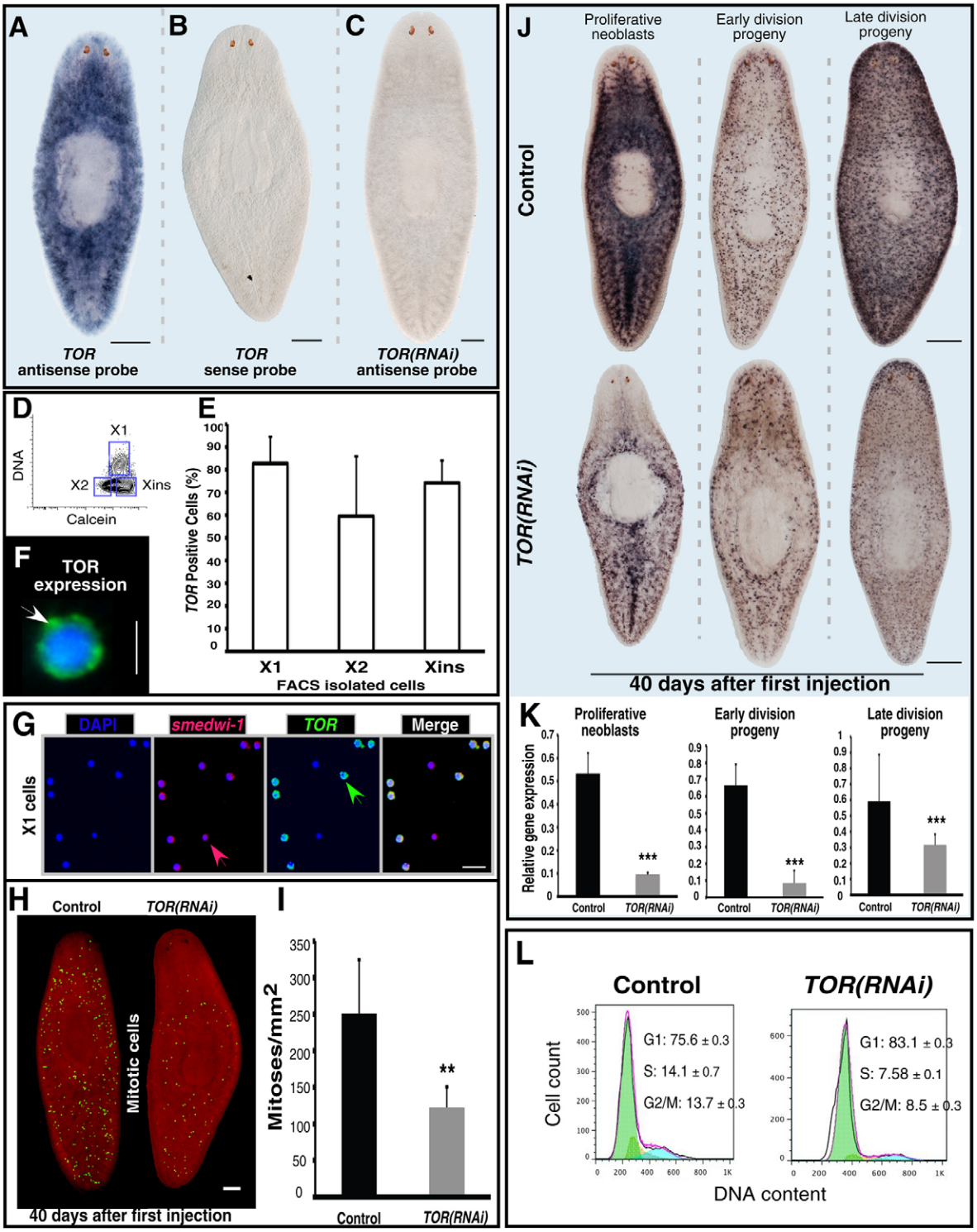

Fig. 1. See next page for legend.

postmitotic progeny (X2), and in differentiated cells (Xins). Furthermore, double-staining ISH determined that a large proportion of proliferative neoblasts co-express both *smedwi-1* and *TOR* (89.2%±7.5 and 82.7±11.7, respectively) (Fig. 1G). Altogether, these experiments demonstrate that *TOR* is widely expressed in neoblasts and differentiated tissues, which is consistent with TOR expression in other organisms (Oldham et al., 2000; Makky et al., 2007).

Systemic inhibition of *TOR* restricts neoblast proliferation

To assess the role *TOR* plays in homeostasis, we designed and optimized a double-stranded RNA (dsRNA) microinjection protocol [*TOR(RNAi)*] that consistently downregulates *TOR* expression throughout the body (Fig. 1C; supplementary material Fig. S2). The RNAi protocol was optimized until it achieved reproducible maximum abrogation (Fig. 1C; supplementary material Fig. S2) in order to reduce the possibility of a *TOR* partial downregulation. Following *TOR(RNAi)*, animals ($n>30$) displayed slower phototactic responses but no lethality 30 days after the first injection. These data suggest that *TOR* is not required for short-term tissue turnover. Under these conditions, strong downregulation of *TOR* gene expression could be achieved in less than a week, but stable effects on neoblasts were detectable ~3 weeks after the first dsRNA injection (see below). This suggests that abnormalities in neoblasts were probably associated with lack of functional TOR protein, and that it takes ~20 days under this RNAi strategy to abolish TOR function in the whole adult worm. Although additional experiments are needed to test for TOR-protein activity, the timelines reported here are consistent with the turnover rate reported for other planarian proteins (Guo et al., 2006; Wenemoser and Reddien, 2010).

To understand the effects of TOR deficiency better, we analyzed neoblast response to cellular turnover. The neoblast is the only proliferative cell in *S. mediterranea* and it can be identified by staining with an anti-phosphorylated histone-3 (H3P) antibody, which labels mitotic neoblasts (Newmark and Sánchez Alvarado, 2000). The mitotic activity in the whole organism was markedly reduced (50%) three weeks after *TOR(RNAi)* (Student's *t*-test, $P<0.0001$), but had not disappeared by 40 days after the first dsRNA injection (Fig. 1H,I). These results indicate that some neoblasts continue to divide even after downregulation of *TOR* signaling, suggesting that neoblast proliferation is not entirely dependent on TOR signaling. This finding is consistent with the reduction in cell proliferation observed after TOR inhibition in some mammalian tissues (Feldman et al., 2009; Shor et al., 2009; Thoreen et al., 2009). Because mitotic cells account for only a limited population of neoblasts, we sought to expand this analysis by including markers that label proliferative, early and late postmitotic progeny of neoblast (*smedwi-1*, *Smed-NB.21.11e* and *Smed-AGAT-1*, respectively) (Eisenhoffer et al., 2008). Similar to mitotic cells, a substantial reduction in expression of proliferative neoblast (82.12%) and early (87.09%) and late (46.60%) postmitotic progeny was sustained over a month after dsRNA injection (Fig. 1J–K). Intriguingly, despite this systemic reduction in cell proliferation, animals survived for >50 days with undetectable *TOR* expression, suggesting that the remaining neoblasts probably contribute to cellular turnover.

The effects of *TOR(RNAi)* on the cell cycle were examined further using flow cytometry by staining nuclei of dissociated cells with DAPI (Fig. 1L). Cell cycle analyses confirmed that downregulation of *TOR* greatly reduces neoblast proliferation (~50%), which is consistent with their mitotic activity as well as the expression of neoblast markers and their progeny (Fig. 1H–K). From these experiments, we concluded that the RNAi strategy applied to abrogate TOR function consistently affects cell cycle dynamics in the neoblast population. Although the reasons for this systemic reduction in cell proliferation are not necessarily clear, it might involve slowing of G1 progression (see increase in the number of cells in G1 and the decrease in G2/M, Fig. 1L) as has been noted in other models with dysfunctional TOR signaling (Pedersen et al., 1997; Feldman et al., 2009; García-Martínez et al., 2009; Shor et al., 2009; Thoreen et al., 2009). Taken together, induction of TOR deficiency with RNAi in planarians provides a simplified model for studying its functions within the complexity of the whole adult organism.

These analyses indicate that *TOR* regulates neoblast proliferation during systemic cell turnover. The reasons for the reduction in proliferative neoblasts and their progeny after TOR-RNAi is not entirely clear, but two possible scenarios could be suggested: (1) TOR inhibition produces a uniform effect on all neoblasts that leads to a gradual decline in their proliferative capacity, and (2) TOR has distinct roles in stem cells along the planarian body, implying that a subset of neoblasts requires this signaling pathway for proliferation whereas some other neoblasts divide independently of TOR. The complexity of the neoblast population is not well understood, but recent evidence supports the notion that intrinsic differences exist among neoblasts (Wagner et al., 2011). TOR inhibition does not produce a uniform cellular response along the mammalian body (Russell et al., 2011), indicating that additional analyses of this phenotype in planarians might shed some light on the systemic regulation of TOR in adult tissues.

Fig. 1. *TOR* is expressed ubiquitously and RNA-interference reduces mitotic activity and expression of neoblast markers. (**A**–**C**) Whole-mount ISH with antisense *TOR* probe shows widespread distribution of *TOR* expression (A). Lack of signal with sense *TOR* probe and antisense *TOR(RNAi)* probe (B–C) demonstrates signal specificity. (**D**) FACS plot shows gates used to isolate irradiation sensitive (X1 and X2) and insensitive (Xins) populations based on viability and the DNA content. (**E**) Bar graph shows TOR-expressing cells are present among neoblasts and differentiated tissues (X1, $n=287$; X2, $n=169$; Xins, $n=380$). No statistical difference is observed between these groups. (**F**) Proliferative neoblast expressing TOR (green). DAPI, blue. (**G**) Double staining with *smedwi-1* and *TOR* fluorescent probes on proliferative cells. The majority of cells co-express both genes. Arrowheads indicate positive signal for each probe. (**H**,**I**) Whole-mount immunostaining with anti-H3P antibody (H) and quantification of mitoses (I) demonstrates reduction in mitotic activity in *TOR(RNAi)* animals (Student's *t*-test, $^{**}P<0.01$). Three independent experiments, $n>12$ animals. (**J**,**K**) *TOR(RNAi)* reduces the expression of the neoblast-associated genes *smedwi-1* (82.12%, proliferative), *NB.21.11* (87.09%, early progeny) and *Smed-AGAT-1* (46.60%, late progeny), which is not necessarily linear with a reduction in the number of cells. Student's *t*-test, $^{***}P<0.001$. qRT-PCR analyses are from triplicated experiments; values represent average and error bars s.d. Gene expressions are relative to the ubiquitously expressed clone *H.55.12e* (Reddien et al., 2005). Whole-mount in situ hybridization consisted of three independent experiments with $n>9$ animals. Scale bars: 200 µm (A–D) and 12.5 µm in dissociated cells (G). (**L**) Cell cycle analysis with DAPI indicates neoblasts progression to cell cycle is impaired after *TOR(RNAi)*, Student's *t*-test G1 phase ($P<0.01$), G2/M phase ($P<0.05$), S phase ($P<0.05$). One representative experiment (mean ± s.d.) of three is shown.

TOR signaling is required for blastema formation but regeneration is accomplished within pre-existing tissues

To investigate the roles of TOR in planarian regeneration, the response to amputation was evaluated in worms subjected to *TOR(RNAi)*. Upon amputation, neoblasts proliferate to form a specialized structure called the regenerating blastema, which is the new tissue from which missing structures are regenerated (Reddien and Sánchez Alvarado, 2004; Gentile et al., 2011). After two rounds of amputation, controls (water injected, $n>40$) regenerated both head and tail within a week, whereas *TOR*-RNAi-treated fragments failed to form recognizable blastemas (95%; Fig. 2A,B). A similar response was also observed after single longitudinal cuts, indicating that this phenotype was not restricted to the number or the type of amputation (supplementary material Fig. S3).

Although neoblasts continue to proliferate after TOR-RNAi, they were unable to form blastema, indicating that TOR signaling is required for blastema formation (Fig. 2A,B). Nonetheless, *TOR*-RNAi fragments without blastemas survived for >40 days after the first injection. Surprisingly, these fragments became sensitive to light and responded to other external stimuli, suggesting that the sensory system was somewhat functional. Over time, *TOR*-RNAi fragments without blastema developed characteristic photoreceptor pigmentation close to the anterior wound. A closer evaluation with nervous system markers revealed an unexpected result: nervous system structures (e.g. brain, visual neurons) removed during amputation were to some extent regenerated in *TOR*-RNAi animals, but within pre-existing tissue (Fig. 2C). These observations indicate that, despite the absence of blastema formation, regeneration in *TOR*-RNAi fragments is not completely suppressed, revealing an intriguing process of regeneration in which nervous tissue is regenerated within pre-existing tissue.

Our data suggest that downregulation of TOR signaling provides an excellent model for identifying mechanisms of injury-induced stem cell response as it specifically prevents blastema formation but does not completely abrogate regeneration. Therefore, we sought to understand better the cellular response to amputation after TOR-RNAi. The initial response of neoblasts to amputation involves two waves of mitoses that are required for blastema formation (Saló and Baguñà, 1984; Wenemoser and Reddien, 2010). Although the molecular signals driving these mitotic waves are unknown, it has recently been shown that the first mitotic peak is a system-wide neoblast response triggered by mechanical injury. This initial wave peaks as early as 6 hours after wounding. The second

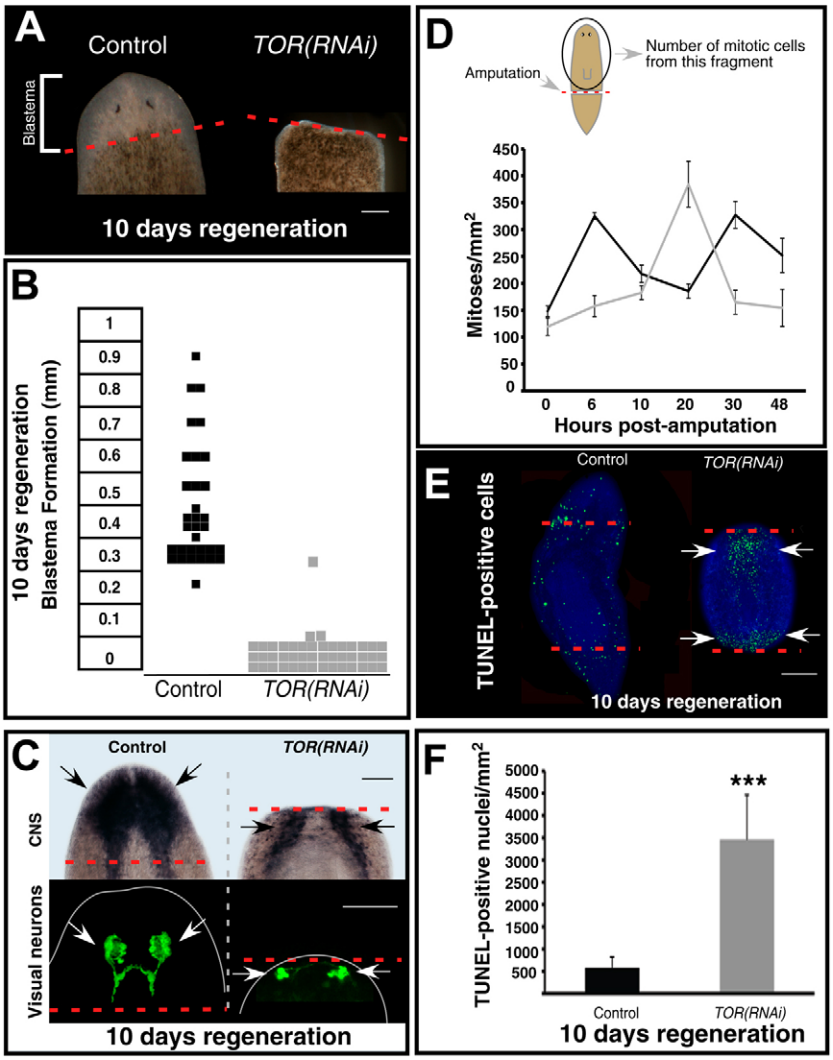

Fig. 2. TOR signaling drives early response of the neoblast to amputation but regeneration occurs in the absence of blastema formation. (**A**) *TOR(RNAi)* prevents blastema formation after two rounds of amputation or in cuts 20 days after first injection. Cephalic regeneration is shown (five independent experiments, $n>180$). Scale bar: 500 µm. (**B**) *TOR(RNAi)* restricts local growth of the blastema ($n>32$ animals). (**C**) Nervous tissue (arrows) that is normally regenerated within the blastema appears in pre-existing tissue after *TOR(RNAi)*. Central nervous system (CNS, *smed-pc2*) and visual neurons (anti-arresting antibody), 10 days after decapitation. Although the mechanism by which brain and visual neurons are regenerated after *TOR(RNAi)* is not necessarily clear, animals sense external stimuli, see text for details ($n>15$, the animal outline is depicted). Scale bar: 200 µm. (**D**) In control animals, two burst of mitoses (at 6 and >30 hours) are triggered after amputation (black line) but in *TOR(RNAi)* only one is observed at 20 hours post-amputation (gray line). The difference in the mitotic response in both groups is statistically significant $P=1.43e\text{-}09$ by two-way-Anova. Each data point represents mean ± s.e.m. of two independent experiments with $n>10$ animals. (**E**,**F**) Apoptosis takes place in absence of functional TOR signaling. The pattern of apoptotic cells remains close to the wounded area and is abnormally increased. TUNEL-positive nuclei are green. In controls, signal is randomly distributed whereas in *TOR(RNAi)* apoptotic cells it is increased (sixfold) and accumulated near the cut surfaces (arrows). Scale bar: 200 µm. Student's *t*-test, $***P<0.0005$. One of two independent experiments ($n=5$ animals) is shown. Red dashed line represents plane of amputation.

mitotic peak, however, is an amputation-induced neoblast response, localized near the wounded area, and is evident ~48 hours after injury (Wenemoser and Reddien, 2010).

Time course regeneration experiments confirmed the post-amputation bimodal mitotic waves that lead to blastema formation in control fragments (Fig. 2D). However, neoblasts in TOR-RNAi worms failed to mount the early systemic mitotic response after amputation (Fig. 2D). Nonetheless, their widespread proliferative response gradually increased to peak 20 hours after amputation, which typically corresponds to the stage of neoblast recruitment and the onset of the local response to loss of tissue (Wenemoser and Reddien, 2010). These results indicate that neoblasts in TOR-RNAi planarians can sense and divide following injury but are unable to reach the proliferative levels required after amputation on time. Whether a second mitotic peak in TOR-RNAi animals occurs 48 hours post-amputation needs to be investigated, but it is unlikely that it affects the process of blastema formation because the initial decisions are made within the first 12–24 hours after injury (Oviedo et al., 2010). Additional experiments are also needed to rule out the mechanism by which neoblasts regenerate missing parts within pre-existing tissues, and whether the lack of blastema is associated with an impaired migratory response to injury within the neoblast progeny. However, we propose that TOR is a crucial component for the signals driving the early widespread neoblast response after amputation (i.e. the first mitotic peak). We speculate that the lack of blastema formation in the absence of TOR signaling could be associated with multiple factors (intrinsic and non-intrinsic) that combine slow proliferative responses in neoblasts upon injury with an impaired migratory property in their progeny.

Spatiotemporal synchronization between cell division and cell death is a requirement for animal regeneration (Hwang et al., 2004; Tseng et al., 2007; Chera et al., 2009; Pellettieri et al., 2010). In planarians, two waves of apoptosis remove differentiated cells after amputation (Pellettieri et al., 2010). Significantly, the time period between the apoptotic peaks overlaps with the neoblast mitotic response. The first apoptotic wave precedes neoblast response to injury and is localized near the wound site. By contrast, the second peak is a systemic cell death response detectable 48 hours post-injury (Gurley et al., 2010; Pellettieri et al., 2010). Apoptosis was evaluated in regenerating fragments by the whole-mount TUNEL method (Pellettieri et al., 2010). Control fragments regenerated and displayed a characteristic apoptotic response pattern similar to that of an uncut animal (i.e. randomly distributed through the body) 7 days post-amputation (Fig. 2E). By contrast, TOR-RNAi fragments consistently displayed an increased and localized cell death response closely associated with the wound surface, even one week post-injury (Fig. 2E). This apoptotic response resembled the distribution pattern of the first wave of apoptosis seen early during regeneration (Pellettieri et al., 2010). Furthermore, amputated *TOR(RNAi)* worms displayed an unexpected sixfold increase in TUNEL-positive nuclei after a week post-amputation (Fig. 2F). These results suggest that cell death induced by regeneration, at least in late stages, takes place independently of TOR signaling. However, the effects of prolonged apoptosis near the wound are unknown.

In 1901, Thomas Hunt Morgan classified animal regeneration into two broad categories: (1) epimorphosis, which requires cell proliferation, and (2) morphallaxis, which proceeds through remodeling of pre-existing tissues and does not entail cellular proliferation (Morgan, 1901). However, after more than a century, the mechanisms regulating each type of tissue repair remain largely unknown (Sánchez Alvarado, 2000; Brockes and Kumar, 2008; Poss, 2010). Our results show that TOR forms part of the endogenous signals essential for blastema formation during epimorphic regeneration. However, in the absence of functional TOR signaling, part of the nervous system regenerates within pre-existing tissues by a process that is not entirely clear. We speculate that it might involve both epimorphosis and morphallaxis. Nevertheless, it reveals TOR signaling to be a key molecular regulator of animal regeneration.

TOR is essential for organismal growth and long-term tissue maintenance but not for remodeling pre-existing tissue

Planarians can increase or decrease their body size according to metabolic and environmental conditions (Baguñà, 1975), although the molecular bases of this remarkable tissue plasticity are unknown. This developmental plasticity in the adult has been associated with addition of new cells during growth, and elimination of specific cells during size reduction (de-growth), which in both cases help to remodel and adjust body proportions accordingly (Oviedo et al., 2003).

The TOR pathway is a sensor that responds to signals, such as nutrient and energy availability, by modulating cell growth and division (Wullschleger et al., 2006; Russell et al., 2011; Zoncu et al., 2011). To test whether *TOR* plays a role in planarian growth and de-growth, we exposed neoblasts to high or low nutrient levels (i.e. continuous feeding or starvation, respectively) and recorded changes in organismal size for 40 days. When maintained under low nutrient levels, control and *TOR(RNAi)* worms decreased in size at the same rate (Fig. 3A). This indicates that tissue remodeling could occur in the absence of functional *TOR*, which is consistent with TOR inhibition under low nutrient conditions observed in other organisms (Zoncu et al., 2011). Indeed, we found that *TOR* expression is downregulated during starvation (supplementary material Fig. S4). Conversely, control animals fed once a week displayed a sustained increase in size, whereas fed *TOR(RNAi)* animals failed to grow and kept their overall size with minimal change for 40 days. Independently of the metabolic status (i.e. starving or feeding) the overall cellular size in *TOR(RNAi)* animals was always smaller than in controls (supplementary material Fig. S5), suggesting that, as in other species, the planarian TOR is a key regulator of cell size (Oldham et al., 2000; Fingar et al., 2002; Fumarola et al., 2005; Zhang et al., 2011). Altogether, these results indicate that TOR signaling is a key molecular component of organismal growth in planarians. This molecular function of TOR could be important for understanding metabolic plasticity during tissue maintenance and regeneration as has been long sought after in the planarian literature (Bardeen, 1901; Morgan, 1901).

The fact that fed *TOR(RNAi)* animals kept their size relatively stable over time is consistent with the notion that the remaining neoblasts to some extent sense nutrients and are capable of supporting tissue turnover (supplementary material Fig. S6). Therefore, the lack of organismal growth in the presence of nutrients, together with the inability of neoblasts to contribute to localized growth after amputation (blastemas, Fig. 2A), suggests that in the absence of functional TOR, the neoblast response to satisfy body demand is restricted, confirming the role of this

pathway as a systemic regulator. Additional experiments are needed to determine whether these effects are the result of a delayed cell cycle transition and/or an altered migratory and differentiation response.

During physiological cell turnover, neoblast division is counterbalanced by programmed cell death (Pellettieri et al., 2010). However, we found that uninjured *TOR(RNAi)* planarians have a 2.5-fold increase in TUNEL-positive nuclei, suggesting that cell division and cell death are not balanced in the absence of functional TOR (Fig. 3B). These data indicate that TOR signaling regulates systemic cell death in planarians, and we propose that an imbalance between systemic neoblast division and cell death probably restricts organismal growth in planarians subjected to *TOR(RNAi)*.

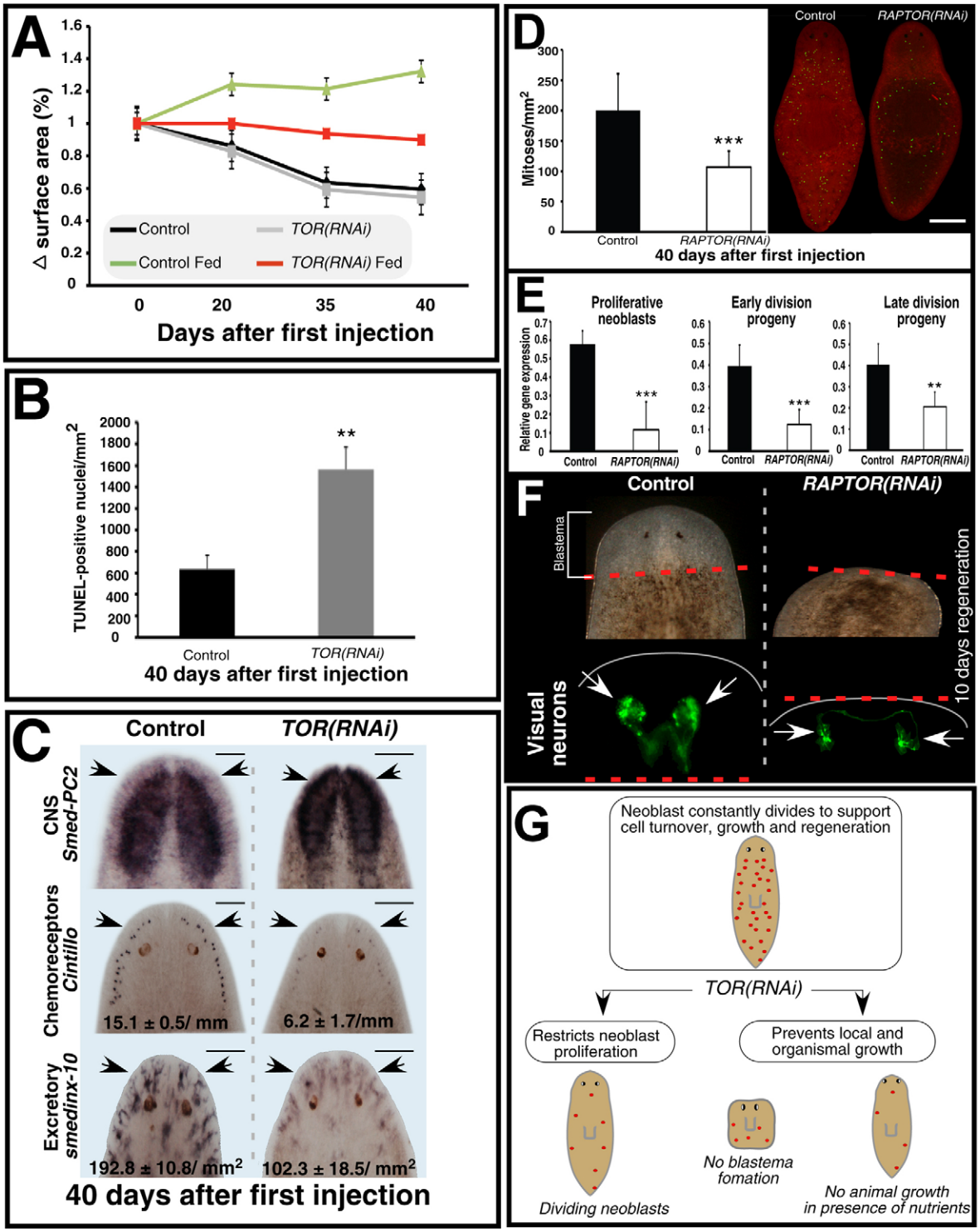

Fig. 3. See next page for legend.

Continuous neoblast division in uninjured planarians supports tissue turnover (Newmark and Sánchez Alvarado, 2000). However, if there is an imbalance between neoblast division and cell death, it might affect long-term tissue maintenance. To test this assumption, the integrity of differentiated tissues was evaluated using organ-specific markers (Fig. 3C). We found that tissue integrity in *TOR(RNAi)* planarians was compromised in at least two ways. First, there was mild loss of tissue (8.7%±1.6 decrease) at the most anterior part, a condition that is known as head regression and is commonly associated with the inability of neoblasts to support tissue turnover (Reddien et al., 2005). Second, the low number of cells expressing the excretory system marker *smedinx-10*, and the allometric indicator *cintillo* suggests that neoblasts in TOR-RNAi animals cannot support long-term systemic tissue turnover (Fig. 3C). We propose that these results, together with high apoptotic levels (Fig. 3B), might lead to the generalized tissue degeneration observed in *TOR(RNAi)* planarians.

RAPTOR, a component of the TOR complex-1, modulates TOR function during tissue homeostasis and regeneration

TOR is the catalytic subunit of two distinct complexes called TOR complex-1 (TORC1) and TORC2 (Wullschleger et al., 2006; Zoncu et al., 2011). Each complex is defined by an accessory protein that is essential for complex assembly: regulatory-associated protein of TOR (RAPTOR) for TORC1 and rapamycin-insensitive companion of TOR (RICTOR) for TORC2 (Zoncu et al., 2011). A homolog sequence for *RICTOR* has not been identified in planarians. However, a highly conserved homolog sequence for RAPTOR (*Smed-RAPTOR*, hereafter referred to as *RAPTOR*) was identified and it displayed a ubiquitous expression pattern resembling that of *pTOR* (supplementary material Fig. S7). *RAPTOR(RNAi)* restricts neoblast division and the expression of neoblast markers (Fig. 3D,E) in a manner consistent with the effects observed after *TOR(RNAi)* treatment (Fig. 1H–K).

The macrolide rapamycin inhibits TOR function through TORC1 (Wullschleger et al., 2006; Zoncu et al., 2011). We found that continuous treatment with rapamycin at >60 nM considerably reduced neoblast division and the expression of neoblast associated genes (*smedwi-1*, *NB.21.11e* and *Smed-Agat-1*) in a similar fashion to *TOR* and *RAPTOR(RNAi)* (Fig. 3D–E; supplementary material Fig. S7). This result suggests that TOR signaling inhibition can be partially recapitulated by targeting only TORC1. Furthermore, *RAPTOR(RNAi)* consistently prevented regeneration in a way that is consistent with both the proposed TOR-protein turnover and the *TOR(RNAi)* phenotype. Moreover, *RAPTOR(RNAi)* amputated worms responded to light stimuli and regenerated visual neurons within pre-existing tissue, resembling the *TOR(RNAi)* phenotype (Fig. 3F). Altogether, aspects of the *TOR(RNAi)* phenotype in planarians can be recapitulated by targeting RAPTOR with either RNAi or treatment with rapamycin (supplementary material Fig. S7), suggesting that the TOR-deficient phenotype described here is likely to be mediated through TORC1. Additional characterization of up- or downstream targets, including AKT, 4E-BP and S6K, present in *S. mediterranea* will provide insights into TOR regulation in adult tissues. Furthermore, analysis using novel TOR inhibitors targeting members of the TORC1 and TORC2 complexes (Feldman et al., 2009; García-Martínez et al., 2009; Shor et al., 2009; Thoreen et al., 2009) has the potential to identify new drug targets to control the behavior of stem cells and to induce tissue-specific regeneration.

Concluding remarks

Taken together, our results reveal that it is possible to perform analysis of TOR function at the systemic level in adult organisms. Furthermore, by applying this paradigm we revealed roles for TOR in controlling adult stem cells during tissue turnover and regeneration (Fig. 3G) that are consistent with effects observed in mammals (Russell et al., 2011; Zoncu et al., 2011). Mammalian cells do not display a uniform response to TOR inhibition but studies on planarians could provide additional opportunities for dissecting complex cell regulation by this pathway in adult tissues. The phenotype described here provides simplified grounds by which the systemic effect resulting from manipulation of ubiquitous signaling pathways could be translated to the complexity of the whole organism. Our results reveal that TOR signaling components are conserved in planarians and that TORC1 probably mediates TOR function during early regenerative response and organismal growth. These findings could enable studies to further characterize epimorphic regeneration without blastema formation. This is of particular interest given that not all regenerative processes involve blastema formation and in some organisms (including humans), tissue repair can take place without the formation of this specialized structure. Our model provides the opportunity to investigate TOR signaling in the whole organism. As the TOR signaling pathway has been the focus of current anticancer therapy, inhibition of TOR function in planarians could also provide unique insights into the consequences of long-term inhibition of this pathway.

Fig. 3. *TOR* is required for organismal growth and long-term tissue maintenance, and its functions are mediated through RAPTOR, a component of TOR Complex-1. (**A**) In *TOR(RNAi)* starvation does not affect 'de-growth' but feeding once a week prevents organismal growth (mean ± s.d. of the percent change (Δ) in surface area, $n=25$ animals/time point); dispersion of data in the *TOR(RNAi)* fed animals is low. Difference in surface area considers length and width of the whole organism. (**B**) Apoptosis is elevated in intact *TOR(RNAi)* animals (Student's *t*-test, $^{**}P<0.005$, two independent experiments, $n>5$). Error bars represent standard deviation. (**C**) Long-term tissue maintenance is not effectively supported after *TOR(RNAi)*. In situ hybridization analysis of *Smed-PC2* (CNS), *cintillo* (chemoreceptors) and *smedinx-10* (excretory) in control and *TOR(RNAi)* worms. About 8.7%±1.6 of tissue is lost between the tip of the animal and the most anterior part of the pigment cups, indicated with arrows in *TOR(RNAi)* but it did not alter *cintillo* quantification. Numbers represent chemoreceptors/mm or cluster of *smedinx-10* associated-signal ± s.d. of three experiments 40 days starvation, $n>8$ animals. Scale bars: 100 µm. Notice the reduction in the expression of *cintillo* and excretory system after *TOR(RNAi)* (Student's *t*-test, $P<0.0001$). All experiments were performed in parallel. (**D**,**E**) A planarian RAPTOR homolog (*RAPTOR*) restricts neoblast division (Student's *t*-test, $P<0.001$) (D), the expression of *smedwi-1* (proliferative, 79.91%), *NB.21.11* (early progeny, 68.73%) and *Smed-Agat-1* (late progeny, 49.09%) (E). Student's *t*-test, $P<0.001$. Scale bar: 200 µm. (**F**) *RAPTOR(RNAi)* prevents blastema formation but induces regeneration of nervous structures within pre-existing tissue (arrows). In each case, two or more experiments with $n>6$ animals. (**G**) Working model illustrating the possibility of following a population of neoblasts that remain proliferating after TOR-RNAi during tissue maintenance and regeneration. *TOR* is an essential component for maintaining homeostasis and regeneration.

Materials and Methods

Identification of homolog and phylogenetic analysis

Homologs for TOR and Raptor were identified in the *S. mediterranea* database SmedDb (Sánchez Alvarado et al., 2002). The sequences were further confirmed by Blastn, blastx, blastp and alignment tools (http://blast.ncbi.nlm.nih.gov/Blast.cgi). A combination of heat repeats and FAT domain were used as molecular signature to identify TOR homologs within the *S. mediterranea* genome (Cantarel et al., 2008; Robb et al., 2008). Reciprocal BLAST analysis identified a single TOR member that was aligned with TOR sequences of other species by using CLUSTALW and T-Coffee software. A predictive evolutionary model was built using MEGA software (www.megasoftware.net).

Planarian culture

Planarian culture was maintained as previously described (Oviedo et al., 2008).

dsRNA and microinjections

dsRNA synthesis and microinjections were carried out as previously described (Oviedo et al., 2008).

TUNEL assay

TUNEL assay was performed as previously described (Pellettieri et al., 2010).

qRT-PCR

RNA extraction and quantitative real-time PCR (qPCR) reactions were performed as previously described (Oviedo et al 2008; Reddien et al., 2005). Briefly, Trizol was used to isolate RNA from control and experimental animals at different times after first dsRNA injection. qPCR reactions were performed using the SYBR Green Master Mix in a 7500 Fast Real Time PCR cycler (Applied Biosystems). All reactions were performed in triplicates using the median cycle threshold value for analysis. Gene expressions are relative to the ubiquitously expressed clone *H.55.12e* (Reddien et al., 2005). See supplementary material Table S1 for primer sequences.

Measurements of planaria and image processing

Animal behavior was recorded using a Nikon AZ-100 multizoom microscope and NIS Elements AR 3.2 software. Automated area measurements were calculated with NIS Elements at day 0, day 20 and day 40 after injection. Standard deviations were obtained by normalizing the area measurements for each set time point to the average on day 0 to obtain percentage standard deviation and this value was divided by the data point to calculate the standard error represented on the graph. Digital pictures were collected using a Nikon AZ-100 multizoom microscope and NIS Elements AR 3.2 software. Brightness and contrast were adjusted with Adobe Photoshop.

FACS

Planarians were dissociated as previously described (Reddien et al., 2005). DAPI was used to stain cell nuclei and the data were collected using an LSRII flow cytometer (BD Biosciences) with DIVA software. Flow cytometry analyses were performed with FlowJo software, Version 8 (www.flowjo.com).

In situ hybridization

Riboprobes for in situ hybridization (ISH) were synthesized using T3 or T7 polymerase (Promega) and digoxigenin-labeled ribonucleotide mix (Roche) with specific PCR templates as previously described (Oviedo et al., 2008). ISH on isolated cells and quantification were performed as previously described (Oviedo et al., 2008). Whole-mount ISH (WISH) was performed as previously described (Pearson et al., 2009).

For ISH on dissociated cells, isolated cells from FACS were spotted onto slides and fixed using 4% paraformaldehyde. ISH was performed as previously described (Oviedo et al., 2008). Propidium iodide (PI) or DAPI were used to stain nuclei. Cells that were double labeled with the nuclei marker and the riboprobe were counted in relationship with the total number of nuclei. Fluorescent in situ hybridization was performed as previously described (Pearson et al., 2009). In all cases, ten different fields were counted per slide.

H3P staining and immunofluorescence

Planarians were fixed and immunostaining performed as previously described (Oviedo et al., 2008). The mitotic cells (H3P positive) were counted and normalized to the area (mm^2) using NIS element software (Nikon). Statistical analyses were performed using Microsoft Excel.

Acknowledgements

We are grateful to Edelweiss Pfister-Oviedo for technical assistance; Liza Gómez-Daglio for assistance with phylogenetic analysis; and Jason Pellettieri, Bret Pearson and Jochen Rink for advice with protocols. We thank Mike Cleary and Sabrina Maisel for comments on the manuscript and Ricardo Zayas, Peter Reddien and Kenji Watanabe for reagents.

Funding

T.H.P. was supported by a Jane Vilas Scholarship and the University of California Merced Graduate Research Council. N.J.O. acknowledges support from the University of California Merced and the University of California Cancer Research Coordinating Committee.

Author contributions

T.H.P., F.W., E.O., D.D., D.R., M.E.G.-O. and N.J.O. performed the research and analyzed the data. N.J.O. conceived the project and wrote the manuscript with T.H.P. and M.E.G.-O.

Supplementary material available online at
http://jcs.biologists.org/lookup/suppl/doi:10.1242/jcs.104711/-/DC1

References

Baguñà, J. (1976). Mitosis in the intact and regenerating planarian *Dugesia mediterranea* n.sp. I. Mitotic studies during growth, feeding and starvation. *J. Exp. Zool.* **195**, 53-64.

Bardeen, C. R. (1901). The function of the brain in Planaria maculata. *Am. J. Physiol.* **5**, 175-179.

Brockes, J. P. and Kumar, A. (2008). Comparative aspects of animal regeneration. *Annu. Rev. Cell Dev. Biol.* **24**, 525-549.

Cantarel, B. L., Korf, I., Robb, S. M., Parra, G., Ross, E., Moore, B., Holt, C., Sánchez Alvarado, A. and Yandell, M. (2008). MAKER: an easy-to-use annotation pipeline designed for emerging model organism genomes. *Genome Res.* **18**, 188-196.

Chera, S., Ghila, L., Dobretz, K., Wenger, Y., Bauer, C., Buzgariu, W., Martinou, J. C. and Galliot, B. (2009). Apoptotic cells provide an unexpected source of Wnt3 signaling to drive hydra head regeneration. *Dev. Cell* **17**, 279-289.

Eisenhoffer, G. T., Kang, H. and Sánchez Alvarado, A. (2008). Molecular analysis of stem cells and their descendants during cell turnover and regeneration in the planarian Schmidtea mediterranea. *Cell Stem Cell* **3**, 327-339.

Feldman, M. E., Apsel, B., Uotila, A., Loewith, R., Knight, Z. A., Ruggero, D. and Shokat, K. M. (2009). Active-site inhibitors of mTOR target rapamycin-resistant outputs of mTORC1 and mTORC2. *PLoS Biol.* **7**, e38.

Fingar, D. C., Salama, S., Tsou, C., Harlow, E. and Blenis, J. (2002). Mammalian cell size is controlled by mTOR and its downstream targets S6K1 and 4EBP1/eIF4E. *Genes Dev.* **16**, 1472-1487.

Fumarola, C., La Monica, S., Alfieri, R. R., Borra, E. and Guidotti, G. G. (2005). Cell size reduction induced by inhibition of the mTOR/S6K-signaling pathway protects Jurkat cells from apoptosis. *Cell Death Differ.* **12**, 1344-1357.

García-Martínez, J. M., Moran, J., Clarke, R. G., Gray, A., Cosulich, S. C., Chresta, C. M. and Alessi, D. R. (2009). Ku-0063794 is a specific inhibitor of the mammalian target of rapamycin (mTOR). *Biochem. J.* **421**, 29-42.

Gentile, L., Cebrià, F. and Bartscherer, K. (2011). The planarian flatworm: an in vivo model for stem cell biology and nervous system regeneration. *Dis. Model. Mech.* **4**, 12-19.

Guo, T., Peters, A. H. and Newmark, P. A. (2006). A Bruno-like gene is required for stem cell maintenance in planarians. *Dev. Cell* **11**, 159-169.

Gurley, K. A., Elliott, S. A., Simakov, O., Schmidt, H. A., Holstein, T. W. and Sánchez Alvarado, A. (2010). Expression of secreted Wnt pathway components reveals unexpected complexity of the planarian amputation response. *Dev. Biol.* **347**, 24-39.

Hwang, J. S., Kobayashi, C., Agata, K., Ikeo, K. and Gojobori, T. (2004). Detection of apoptosis during planarian regeneration by the expression of apoptosis-related genes and TUNEL assay. *Gene* **333**, 15-25.

LaFever, L., Feoktistov, A., Hsu, H. J. and Drummond-Barbosa, D. (2010). Specific roles of Target of rapamycin in the control of stem cells and their progeny in the Drosophila ovary. *Development* **137**, 2117-2126.

Makky, K., Tekiela, J. and Mayer, A. N. (2007). Target of rapamycin (TOR) signaling controls epithelial morphogenesis in the vertebrate intestine. *Dev. Biol.* **303**, 501-513.

Morgan, T. H. (1901). *Regeneration*. New York: The Macmillan Company.

Murakami, M., Ichisaka, T., Maeda, M., Oshiro, N., Hara, K., Edenhofer, F., Kiyama, H., Yonezawa, K. and Yamanaka, S. (2004). mTOR is essential for growth and proliferation in early mouse embryos and embryonic stem cells. *Mol. Cell. Biol.* **24**, 6710-6718.

Newmark, P. A. and Sánchez Alvarado, A. (2000). Bromodeoxyuridine specifically labels the regenerative stem cells of planarians. *Dev. Biol.* **220**, 142-153.

Oldham, S., Montagne, J., Radimerski, T., Thomas, G. and Hafen, E. (2000). Genetic and biochemical characterization of dTOR, the Drosophila homolog of the target of rapamycin. *Genes Dev.* **14**, 2689-2694.

Oviedo, N. J., Newmark, P. A. and Sánchez Alvarado, A. (2003). Allometric scaling and proportion regulation in the freshwater planarian Schmidtea mediterranea. *Dev. Dyn.* **226**, 326-333.

Oviedo, N. J., Pearson, B. J., Levin, M. and Sánchez Alvarado, A. (2008). Planarian PTEN homologs regulate stem cells and regeneration through TOR signaling. *Dis. Model. Mech.* **1**, 131-143, discussion 141.

Oviedo, N. J., Morokuma, J., Walentek, P., Kema, I. P., Gu, M. B., Ahn, J. M., Hwang, J. S., Gojobori, T. and Levin, M. (2010). Long-range neural and gap junction protein-mediated cues control polarity during planarian regeneration. *Dev. Biol.* **339**, 188-199.

Pearson, B. J., Eisenhoffer, G. T., Gurley, K. A., Rink, J. C., Miller, D. E. and Sánchez Alvarado, A. (2009). Formaldehyde-based whole-mount in situ hybridization method for planarians. *Dev. Dyn.* **238**, 443-450.

Pedersen, S., Celis, J. E., Nielsen, J., Christiansen, J. and Nielsen, F. C. (1997). Distinct repression of translation by wortmannin and rapamycin. *Eur. J. Biochem.* **247**, 449-456.

Pellettieri, J., Fitzgerald, P., Watanabe, S., Mancuso, J., Green, D. R. and Sánchez Alvarado, A. (2010). Cell death and tissue remodeling in planarian regeneration. *Dev. Biol.* **338**, 76-85.

Poss, K. D. (2010). Advances in understanding tissue regenerative capacity and mechanisms in animals. *Nat. Rev. Genet.* **11**, 710-722.

Reddien, P. W. and Sánchez Alvarado, A. (2004). Fundamentals of planarian regeneration. *Annu. Rev. Cell Dev. Biol.* **20**, 725-757.

Reddien, P. W., Oviedo, N. J., Jennings, J. R., Jenkin, J. C. and Sánchez Alvarado, A. (2005). SMEDWI-2 is a PIWI-like protein that regulates planarian stem cells. *Science* **310**, 1327-1330.

Robb, S. M., Ross, E. and Sánchez Alvarado, A. (2008). SmedGD: the Schmidtea mediterranea genome database. *Nucleic Acids Res.* **36**, D599-D606.

Russell, R. C., Fang, C. and Guan, K. L. (2011). An emerging role for TOR signaling in mammalian tissue and stem cell physiology. *Development* **138**, 3343-3356.

Saló, E. and Baguñà, J. (1984). Regeneration and pattern formation in planarians. I. The pattern of mitosis in anterior and posterior regeneration in Dugesia (G) tigrina, and a new proposal for blastema formation. *J. Embryol. Exp. Morphol.* **83**, 63-80.

Sánchez Alvarado, A. (2000). Regeneration in the metazoans: why does it happen? *Bioessays* **22**, 578-590.

Sánchez Alvarado, A., Newmark, P. A., Robb, S. M. and Juste, R. (2002). The Schmidtea mediterranea database as a molecular resource for studying platyhelminthes, stem cells and regeneration. *Development* **129**, 5659-5665.

Shor, B., Gibbons, J. J., Abraham, R. T. and Yu, K. (2009). Targeting mTOR globally in cancer: thinking beyond rapamycin. *Cell Cycle* **8**, 3831-3837.

Thoreen, C. C., Kang, S. A., Chang, J. W., Liu, Q., Zhang, J., Gao, Y., Reichling, L. J., Sim, T., Sabatini, D. M. and Gray, N. S. (2009). An ATP-competitive mammalian target of rapamycin inhibitor reveals rapamycin-resistant functions of mTORC1. *J. Biol. Chem.* **284**, 8023-8032.

Tseng, A. S., Adams, D. S., Qiu, D., Koustubhan, P. and Levin, M. (2007). Apoptosis is required during early stages of tail regeneration in Xenopus laevis. *Dev. Biol.* **301**, 62-69.

Wagner, D. E., Wang, I. E. and Reddien, P. W. (2011). Clonogenic neoblasts are pluripotent adult stem cells that underlie planarian regeneration. *Science* **332**, 811-816.

Wenemoser, D. and Reddien, P. W. (2010). Planarian regeneration involves distinct stem cell responses to wounds and tissue absence. *Dev. Biol.* **344**, 979-991.

Wullschleger, S., Loewith, R. and Hall, M. N. (2006). TOR signaling in growth and metabolism. *Cell* **124**, 471-484.

Zhang, S., Readinger, J. A., DuBois, W., Janka-Junttila, M., Robinson, R., Pruitt, M., Bliskovsky, V., Wu, J. Z., Sakakibara, K., Patel, J. et al. (2011). Constitutive reductions in mTOR alter cell size, immune cell development, and antibody production. *Blood* **117**, 1228-1238.

Zoncu, R., Efeyan, A. and Sabatini, D. M. (2011). mTOR: from growth signal integration to cancer, diabetes and ageing. *Nat. Rev. Mol. Cell Biol.* **12**, 21-35.

Journal of Cell Science